Towards an Integrated Low-Cost Agricultural Monitoring System with Unmanned Aircraft System

Georgios D. Karatzinis, Savvas D. Apostolidis, Athanasios Ch. Kapoutsis, Liza Panagiotopoulou,
Yiannis S. Boutalis, Elias B. Kosmatopoulos

Abstract— **Over the last years, an intensified interest has been shown in many studies for precision agriculture. Unmanned Aircraft Systems (UASs) are capable of solving a plethora of surveying tasks due to their flexibility, independence and customization. The incorporation of UASs remote sensing in precision agriculture enhances the abilities of crop mapping, management and identification through vegetation indices. In addition to this, different image analysis and computer vision processes were adopted trying to facilitate field operations in cooperation with human intervention to enhance the overall performance. In this paper, we present a practically oriented application on vineyards towards an integrated low-cost system which utilizes Spiral-STC (Spanning Tree Coverage) algorithm as a Coverage Path Planning (CPP) method. Based on the resulted flight campaign, UAV images were collected, and the incorporated image analysis processes finally extract vegetation knowledge. Also, geo referenced orthophotos and computer vision applications complete the generated oversight of the field. These supportive tools provide farmers with useful information (crop health indicators, weather predictions) letting them extrapolate knowledge and identify crop irregularities.**

I. INTRODUCTION

Unmanned Aircraft Systems (UASs) also referred to as Unmanned Aerial Vehicles (UAVs) and drones, present a continuous expanding key role in different applications [1]. Their adoption in the field of agriculture bodes a promising factor and probably a well-established core asset-component in the future with multiple benefits. Over the last decades, a variety of applications are directly connected with precision agriculture as a result of many technological advances and engineering innovations providing economic and environmental benefits [2], [3]. These technologies incorporate sensors (soil, crop, field, yield etc), controls (automatic guidance systems, robotic harvesting systems, networked systems etc) and information management systems (GIS packages and data interchange standardization). In addition to this, the miniaturization of individual components such as microprocessors, sensors, batteries, communication devices as well as their cost reduction led to the introduction of UAS as remote sensing platforms gathering extensive amounts of raw data [4].

Georgios D. Karatzinis, Savvas Apostolidis, Yiannis S. Boutalis and Elias B. Kosmatopoulos are with the Dept. of Electrical and Computer Engineering, Democritus University of Thrace, Xanthi, 67100, Greece, {gkaratzi,sapostol,ybout,kosmatop}@ee.duth.gr.

Athanasios Ch. Kapoutsis is with the Information Technologies Institute, Centre for Research & Technology, Hellas (ITI-CERTH), Thessaloniki, 57001, Greece, athakapo@iti.gr.

Liza Panagiotopoulou is with GEOTOPOS S.A., Athens, 15343, Greece, lizapan@geotopos.gr.

UAV remote sensing platforms present strong benefits as compared with traditional piloted aircrafts and satellites due to their increased flexibility and easy deployment satisfying requirements of rapid monitoring, assessment and mapping in natural resources [5]. They have established and preferred in comparison with their predecessors as they provide much safer and cost-efficient ways for data acquisition with better abilities of acquiring detailed images at different lighting conditions and flight altitudes. Generally, UAV-based image sensing as an alternative geo-data acquisition method exhibits a well-accepted trade-off between flexibility, high resolution, low-cost and limited flight time (low battery lifetime), small coverage. A comparative study [6] resulted that with respect to aircraft and satellite, UAVs can operate closer to the target and their flexibility on scheduling, acquisition on cloud cover conditions, resolution and precision were identified-classified as optimal. On the contrary, the attributes associated with the coverage range, flight endurance and mosaicking and geocoding effort were characterized as poor.

A complete UAV remote sensing system consists basically of: 1) sensors, 2) auto pilot system, 3) inertial measurement unit (IMU), 4) global positioning system (GPS), 5) data link and 6) ground station. These core components are used for data acquisition, control of the aircraft, as attitude measurement and heading reference system for aircraft maneuvering, navigation, data transfer and mission monitoring/information interaction components respectively. Acquisition sensors may vary between an extended list of RGB, multispectral and hyperspectral cameras, Light Detection and Ranging equipment (LiDAR) etc. However, there is a continuous increased interest for low-cost visual band cameras in comparison with LiDAR systems, as Structure from Motion (SfM) techniques provide the ability to create 3D reconstructions from 2D images and extract useful profile information. The construction processes of 2D orthomosaics and 3D canopy surface models are of particular importance in accurate crop mapping and canopy detection.

Useful information for the under-investigation areas can be extracted also from vegetation indices (VI). This is a valid way to measure the overall amount and quality of photosynthetic material and present farmers and agriculturalists with the field's profile. Indicative applications associated with agricultural operations/tasks include chlorophyll content mapping of corn [7], rice growth and grain yield estimation [8], discrimination of vegetation in wheat fields [9], detecting vegetation rows in vineyards [10]. Vineyards especially are one of the main domains of agriculture in Greece. Moreover, Greece is one of the major country producers of wine and wine grapes (fresh, table,
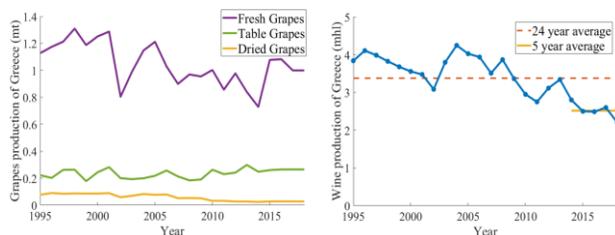
Figure 1. Evolution of grapes (left) and wine (right) production of Greece for the period 1995-2018.

dried) with a total vine area of 106kha (2018 register). The wine improvement in terms of quantity and quality is very important for the development of the primary agriculture sector and the contribution to the national economy.

However, according to the 2019 statistical report published by the International Organisation of Vine and Wine [11], the production volume of Greece for the year 2018 evaluated at 2.2mhl presenting an overall decrease of 15% compared with the 2017 produced volume, while the total vineyard surface area the last 10 years is quite similar. In contrast with the major wine producers inside EU, Greece records a lower than its 5-year average (-12.6%) and a disappointing historical low -35% decline with respect to the 24-year average as presented in Fig. 1. The reported results show the existence of indubitably needs of viniculture in Greece and define the clear future requirements of key actions. The significance of the above results rises even more for canopy regions covered with Protected Designation of Origin (PDO) and Protected Geographical Indication (PGI) which are strictly connected with their geographical origin. By applying autonomous precision operations, we can mitigate this problem by improving the stability and sustainability of production with multiple positive benefits and further enhancements. In addition to the improvements in the management and efficiency, the establishment of such methodologies will significantly reduce the environmental footprint of extensive agriculture activities. Therefore, vineyard mapping in combination with utilities such as to access vegetation state, monitor the canopy vigour and get updates about possible erosion or flood, define decisive factor of future enhancement. The condition factors in conjunction with computer vision processes are getting more essential in crop monitoring. These give an increased meaning to proactive actions on stressed plants and in fact alleviate the smooth farm operations and improve sustainability. The overall enhancement rises in terms of quantity and quality of production, energy saving, manpower reduction, crop management and growth optimization and costs reduction.

Due to the defined needs and the aforementioned possible benefits, the current paper aims at an efficient threefold embrace of a Spiral Spanning Tree coverage algorithm, traditional condition factors and computer vision processes incorporated in a uniform way. The material of the paper is organized as follows: In Section II a brief literature review and the general campaign workflow are presented. Section III analyses the path planning coverage requirements and the adopted method. Section IV describes the off-line post-processing image analysis and the produced results. Finally,

Section V outlines the conclusions and future remarks for upcoming improvements.

II. RELATED WORK AND MATERIAL DESCRIPTION

An identified frontline goal in precision agriculture is the reliable incorporation of UAV and UGV systems in continuous management and monitoring processes. This way a recurrent set of crop profile information provides useful effort for plant health monitoring guiding to proper actions for improving or sustaining the health level. At the same time, this is essential for planning regular agricultural works such as seeding, pruning, fertilizing, spraying and harvesting.

A. Related Work

In order to achieve these benefits, three main categories/scenarios according to the nature of robots, characterize the implementations related to existing literature. The case studies concern i) only UAV-based systems, ii) UGV alone and iii) UAV+UGV working symbiotically and synergistically. A dedicated method was developed in [12] to estimate several vineyard characteristics using the RGB method imagery acquired from an unmanned aerial vehicle (UAV) platform. The included features were row orientation, height, width and row spacing, as well as canopy cover fraction and percentage of missing row segments. Other works incorporate multispectral images and vegetation indices for cultivation analysis [13], [14]. The use of both multispectral and thermal cameras onboard of an UAV led to assessment of vineyard water status as presented in [15]. In fact, high correlations were found between indices based on thermal and on multispectral images with vineyard water status. An UAV could be used to assess vine water status and to map within vineyard variability, which could be useful for irrigation practices.

In the case of UGV alone systems, many research studies are dedicated in automatic grape detection and precision picking trying to distinguish fruits from background. Luo et al. [16] used RGB images to extract multiple effective color components from YCbCr, HSI and L*a*b transformation. The effective color components were extracted based on a thresholding methodology to construct weak classification models. A strong classifier performing grape detection was constructed using the AdaBoost algorithm, by assembling the weak classifiers. Finally, morphological filtering and morphological region filling procedures were applied to eliminate the remaining noise and fill the holes in the image respectively and the enclosing rectangle method completes the framework by marking the clusters. Other works try combining color and texturing features to enhance the overall fruit detection procedure. A work which follows this philosophy has been presented in [17], accelerating fruit detection by isolating and counting bunches in grapes. Experiments performed on two varieties of red grapes, Shiraz and Cabernet Sauvignon, resulting a detection accuracy of 88%. An algorithm for grape clustering and foliage detection and localization for autonomous selective vineyard sprayer was proposed in [18].

Instead of using the UAV or UGV system alone, a scenario in which the two types of robots form a symbiotic system was proposed in [19]. The UAV can land on the UGV, and the UGV transports the UAV between deployment

locations. In the same work, the authors show how to plan the motion of this symbiotic UAV+UGV system on a metric graph, which allows them to apply orienteering algorithms. An interesting work of aerial-ground collaborative 3D mapping is presented in [20]. The problem is analyzed in a cooperative UAV+UGV multimodal environment representation where maps built from both robots and the data association problem is casted as a large displacement dense optical flow estimation.

B. UAV Campaigns and Material

The field images were acquired by a light-weight quadcopter DJI Phantom 4 Pro and 3DR Solo in two distinct scenarios for cotton and vineyard monitoring. Also, the total area of the under-investigation fields is approximately 4.9ha and 1.25ha respectively. The first study area was covered by the DJI Phantom R Pro mounted camera (FC6310), while for the second study the Parrot Sequoia multispectral camera was used. The cotton flight campaign was managed mainly for evaluating the path planning coverage procedure that will be described in Section III. Useful flight information details are presented in Table I including camera specifications, flight attributes, overlap percentage and GSD (ground sampling distance). Having substantial forward and side overlap alleviates procedures of stitching acquired images and as a result to obtain satisfactory reconstruction results. The above parameters may vary according to the goal of the flight campaign. Indicatively, parameters such as flight altitude, overlap and GSD are highly dependent based on the goal of the flight. A detailed 3D model generation requires small distance between two consecutive pixel centers measured on the ground, which means low flight altitude and high overlap. In contrast, applications aimed at monitoring and management of crops can be accomplished at lower resolution from a higher and wider point of view.

Following the above flight parameters, the general workflow scheme of UAV-based remote sensing system is utilized in Fig. 2. Three base phases constitute the flight preparation, planning and post-processing subsystems and complete the pipeline of the system. Firstly, devices and general parameters are specified. Proper specifications of area of interest, camera information and longitudinal and transversal overlap are required for generating flight planning. The last subsystem is responsible for off-line data post- processing and visualization purposes. The exported
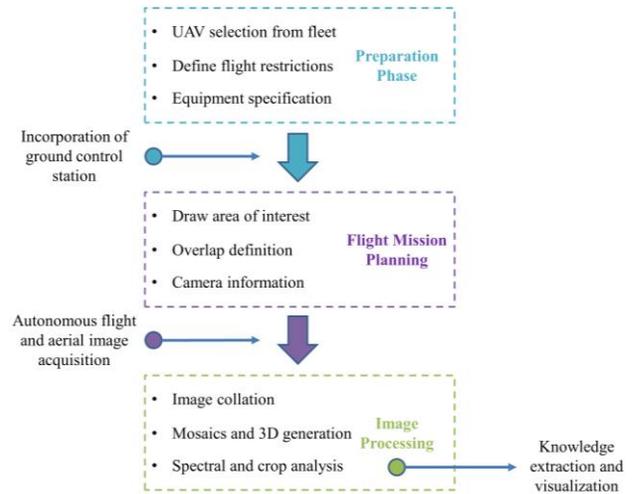

Figure 2.   General workflow scheme of UAV-based remote sensing system.

results are capable for providing crop management and monitoring properties. This is achieved through valuable vegetation indices and processes of image segmentation. Ground control station takes part during mission planning as well during flight as a platform for specifying parameters, tele-control and real-time observation.

III.   PATH PLANNING COVERAGE PROCEDURE

The coverage path planning (CPP) problem is the task of determining a path that passes over all points of an area or volume of interest while avoiding obstacles. A comprehensive survey has investigated the existing coverage path planning methods in 2D environments [21].

A. Requirements

To properly design the path planning algorithm, at first, we should identify the key aspects that determine the performance of a coverage task. Taking into consideration that usually the fields do not have a standard geometry, any adopted path planning solution should be able to design UAV's trajectories that completely cover arbitrary, non-convex polygons. On top of that, in many fields there are some sub-regions, where either a coverage is not useful (e.g. different variety of plants) or it is not safe to perform a flight above them (e.g. personnel or farming equipment is placed in this area). Therefore, the path planning methodology should be able to cope with such no-fly zones and exclude them from the produced trajectory.

Additionally, the scan should be completed in the minimum possible time. This minimum possible time constraint, at first, allows the operator to minimize the waiting time on the field, which can be a really tedious procedure. However, the most important reason, for the optimization with the respect to the coverage time, is the optimal utilization of the UAV's battery. The number one bottleneck for almost all the UAV's operation is the battery time [22], therefore an improved – in terms of coverage time – plan can play a crucial role in the final area of coverage with the existing infrastructure. It is worth highlighting that the improvements that come with the acquisition of more UAVs, spare batteries or docking/charging stations can be

TABLE I.   FLIGHT CAMPAIGN INFORMATION

Species	Cotton	Vineyard	
Flight Date	12/9/2019	29/7/2019	
Growth Stage	Boll opening	Veraison and fruit maturation	
Flight Height (m)	50	80	
Speed (m/s)	3	4.5	
Overlap (%) Side/Forward	80/80	80/85	
Image Size (pixels)	5472x3078 (RGB)	4608x3456 (RGB)	1280x960 (Monochrome)
Sensor size (mm)	13.2x8.8	6.17x4.63	4.8x3.6
GSD (cm/pix)	1.37	2.2	7.5

significantly amplified, if an optimal path planning algorithm is also adopted. Overall, the trajectory of the UAV should i) completely cover the user-defined parts of field with the desired accuracy, ii) without backtracking in already visited areas, and iii) start the operation from its exact initial position, i.e. does not need any preparatory stage.

B. Adopted Solution

To accomplish the aforementioned features an algorithm based on the Spanning Tree Coverage (STC) methodology [23] was adopted. This solution is an O(n) algorithm, where n denotes the size of the field, capable of constructing the minimum path that covers the whole field, starting from any arbitrary point.

The main steps of this procedure are outlined in figure 3. Fig. 3 (a) illustrates the first part of this algorithm, which is the discretization of the field into cells that have the size of the desired coverage accuracy. The no-fly areas of the field are represented with black cells. Fig. 3 (b) graphically illustrates the transition from cells to nodes, i.e. one node is placed for every 4 cells. The nodes that correspond to obstacles are discarded from the graph and in all nodes are added that edges that correspond to the Von Neumann neighborhood. At this stage (figure 3 (c)), we have converted the initial operational area into a fully connected graph. As next step, the number of edges in this graph is reduced, by applying a minimum spanning tree methodology (e.g.

(a) Discretization of the field   (b) Convert cells to nodes

(c) Discard the nodes that correspond to obstacles and add the edges   (d) Construct a Minimum Spanning Tree

(e) The resulting MST is our guide for the navigation   (f) The final path tha circumnavigates the MST
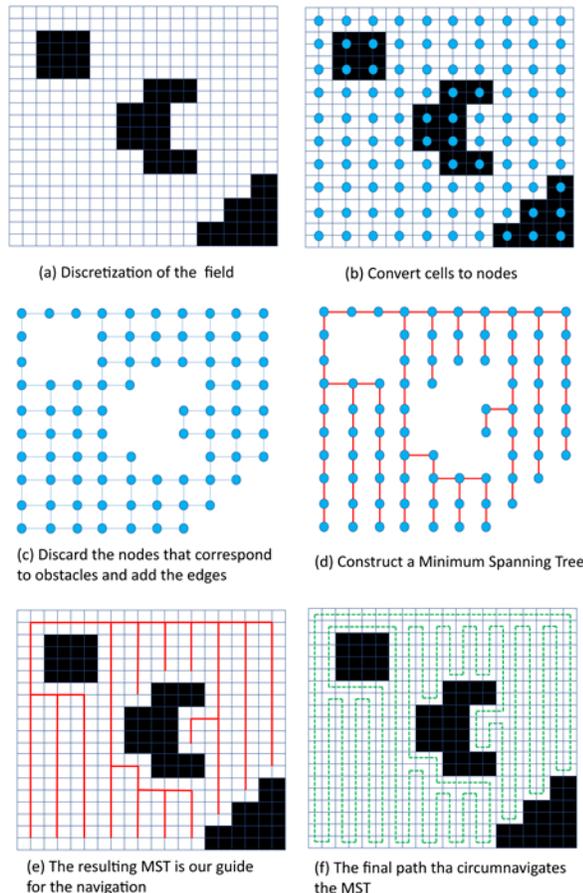
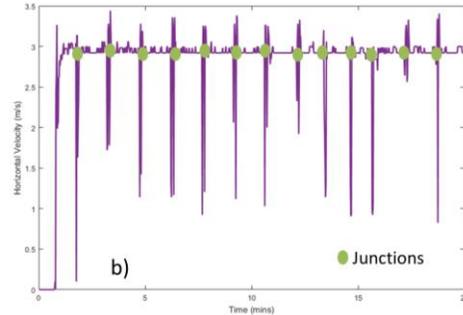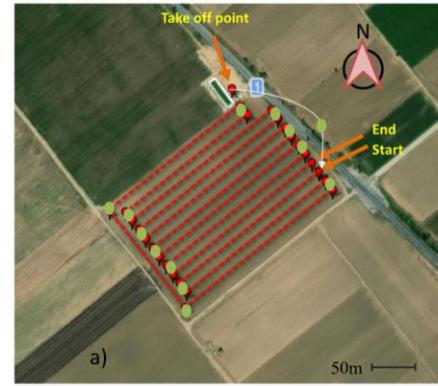Figure 3.   Spanning Tree Coverage Algorithm – Key steps.

Figure 4.   a) Flight path planning, b) horizontal velocity.

Kruskal or Prim [24]). The reduced graph, which is illustrated in figure 3 (d), has the minimum number of edges that are necessary, so as the graph to remain fully connected. Figure 3 (e) graphically illustrates the previously calculated spanning tree on top of the original discretized area. The purpose of this illustration is to highlight that this minimum spanning tree serves as a "guide" for the UAV.

Fig. 3 (f) presents the final path for the UAV that has been calculated by circumnavigating this spanning tree. The produced trajectory completely covers the desired parts of the field, without backtracking into previously covered regions, takes into consideration the initial position of the UAV and finally the return of the UAV to the starting position (usually the base) is part of the coverage plan itself. The aforementioned methodology was implemented and evaluated at a cotton field as mentioned in Section II. Fig. 4 (a) illustrates the resulting path plan for a 4.9ha area, while Fig. 4 (b) presents the horizontal velocity variations during the flight from the take off point to the "End" state. The produced path is constituted by 14 lines including the distance covered from take-off point to the "Start" point. Green dots represent nodes between lines in which the UAV turns, in order to "catch" the route between waypoints.

IV.   DATA ANALYSIS AND IMAGE PROCESSING

This section describes the off-line image processing implementation including actions of crop identification, health evaluation, segmentation and row detection. The under-investigation vineyard is depicted in Fig. 5. It consists of three different varieties (A: Savvatiano, B: Malagousia, C: Assyrtiko). The captured overlapping RGB images, taken from an automatically generated path as described in the

Figure 5.   Vineyard study area, view from satellite. Three sub cultivated areas with different vineyard species.A: Savvatiano, B: Malagousia, C: Assyrtiko. D stands for the cultivated area that will be used in the next subsections.

Figure 6.   Generated orthomosaic for the study area using the acquired RGB images.

previous section, were used in order to generate the resulting panorama. Specialized procedure for creating orthophoto includes feature extraction; feature matching; mismatch removal; image blending and fusion. More specifically, the first step assumes SIFT features extracted from all images for detecting keypoints. Then, feature matching procedure finds most similar features between images finds the relation between images. Taking into consideration the matched feature vectors, RANSAC algorithm computes the homography between images. This way RANSAC selects inliers that are consistently related with a homography and finds a solution that has the best consensus with the data. After removing exterior points, image blending introduces an interpolation procedure in order to be ensured that the resulted image presents zero transition with respect to the source images. Fig. 6 illustrates the orthomosaic representation of the vineyard area as calculated by the aforementioned procedure.

A.   Spectral Indices and Image Segmentation

Vegetation indices (VI) are widely used for evaluating vegetation areas in terms of quality and quantity as they utilize spectral information. The spectral response of the investigated surface is transformed into reliable and interpretable formulas that identify and discriminate plant biomass from soil and other exogenous to the vegetation elements. A variety of methods have been proposed in the literature using RGB and multispectral camera sensors. Also, hyperspectral sensors provide even more bands compared with multispectral, in the range of hundreds to thousands narrow bands. More narrow bands increase the level of spectral detail and the produced indices result in better correlation with crop photosynthetic activity. Broadband and narrowband VIs are suitable for precision agriculture procedures and they are distinguished based on the reflectance bands they use. Both VI categories present ability to estimate the green vegetation cover and the quality of the photosynthetic material. In general, narrowband indices may provide slightly better capabilities of identifying the vegetation biophysical parameters, mainly in areas with dense vegetation, as they present higher level of sensitivity [4].

The incorporation of color-based indices allows humans to identify naturally the greenness part. The most known color based indices include i) Excess Green Index (ExG) [25], Green Leaf Index (GLI) [26], Normalized Green Red Difference Index (NGRDI) [27] calculated directly from RGB images, ii) using Hue-Saturation (HS) and Hue (H) color spaces [28] and iii) LAB colour space [29]. Excess Green Index is computed as follows:

$$ExG = 2G^* - R^* - B^* \qquad (1)$$

where the chromatic coordinates R^*, G^*, B^* are:

$$R^* = \frac{R}{R+G+B}, \; G^* = \frac{G}{R+G+B}, \; B^* = \frac{B}{R+G+B} \qquad (2)$$

where R, G and B are the normalized values in the range [0, 1] and these coordinates can be obtained from:

$$R = \frac{R_c}{R_m}, \; G = \frac{G_c}{G_m}, \; B = \frac{B_c}{B_m} \qquad (3)$$

with R_c, G_c, B_c are the actual pixel values and R_m, G_m, B_m are the maximum values and equal with 255.

Normalized Difference Vegetation Index (NDVI) [30] has claimed a dominant role in remote sensing using the near infrared spectrum. This index highlights the vegetative status and the existing crop biomass with high accuracy from multispectral and hyperspectral remotely sensed images. This is because plants emit part of the absorbed solar radiation in the near infrared region. In other words, the signature of the vegetation reflectance is reflected in the near-infrared (NIR) and the vegetation absorption in the red band. Therefore, NDVI is computed from:

$$NDVI = \frac{NIR - R}{NIR + R} \qquad (4)$$

NDVI values are limited in the interval [-1,1]. The NDVI

range is unfolded in agronomic values revealing the surface type. A practical classification of these values is: i) values from -1 to 0 indicate generally water, snow or cloud existence, ii) values between 0 - 0.2 indicate soil, barren land and rocks while iii) values above 0.2 indicate vegetation with higher canopy cover as approaching 1. The vigor map of the vineyard using NDVI is presented in Fig. 7, while a zoomed view of the vineyard with soil excluded is depicted in Fig. 8.

In order to identify vegetation and separate plants from the background we examine three methods for image segmentation purposes using the RGB images captured during flight. The first step is to use decorrelation stretching in order to enhance and exaggerate color differences. In the first two approaches we convert the images from the RGB color space into HSV and L*a*b* color spaces respectively. At the HSV color spectrum, Hue channel expresses the color component in degrees range: red from 0° to 60°, yellow from 61° to 120°, green from 121° to 180°, cyan from 181° to 240°, blue from 241° to 300° and finally magenta from 301° to 360°. Saturation represents the amount of gray measured in percentage and the value channel represents the brightness or intensity of the color, from 0% (black) to 100% (brightest level).
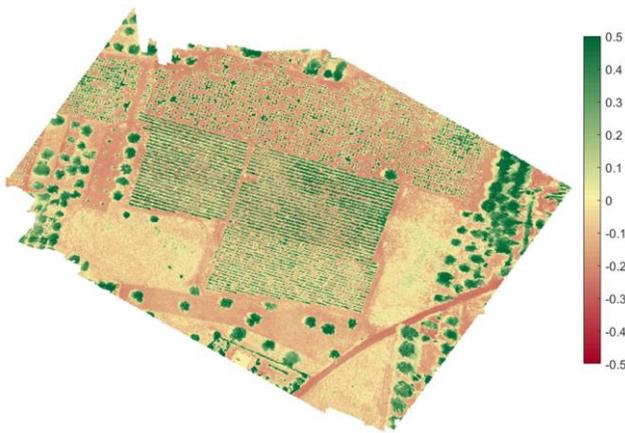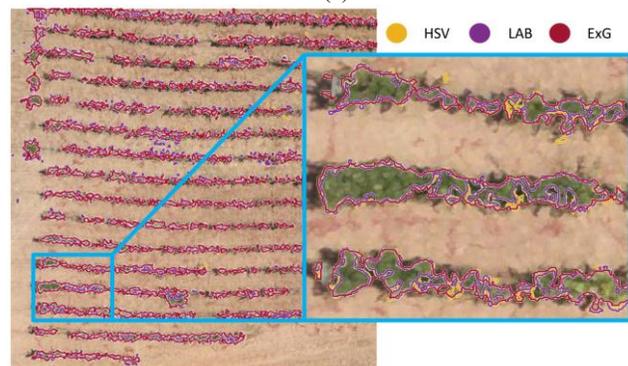
In the CIE L*a*b* color space, L* component stands for the lightness value from 0 (dark) to 100 (bright) while a* and b* represent the color channels. The a* axis describes the green-red component with negative values referring to green and positive to red chromatic components. Similarly, b* axis values move towards blue to yellow color components from negative to positive.

The third approach is dedicated to the incorporation of ExG index, where the equations described in (1)-(3) were implemented in the resulted image after the decorrelation stretch. Then, the vegetation mask was obtained using appropriate threshold to transform the grayscale image into a binary image.

A well-known technique for discrimination of two different classes is the automatic Otsu's thresholding method [31]. In this case, Otsu thresholding is used to extract plant objects and discriminate them from soil and other exogenous elements. Following the aforementioned procedures, vine canopy identification and segmentation was evaluated at the selected area D as noted in Fig. 5. The HSV thresholds for the selected segments were defined: $H_{min}=0.2$, $H_{max}=0.45$; $S_{min}=0.6$, $S_{max}=1$; $V_{min}=0.2$, $V_{max}=1$. For the case referred to L*a*b* color space: $a^*_{min}=-100$, $a^*_{max}=-25$; $b^*_{min}=15$, $b^*_{max}=100$. Fig. 9 utilizes the segmentation results for an indicative sub-area of D using the three aforementioned methods. The under-investigation area was annotated manually (see Fig. 9(a)). A visual interpretation of the result is represented in Fig. 9(b) for the selected area, while the

Figure 7. Vigor map of the vineyard using NDVI.
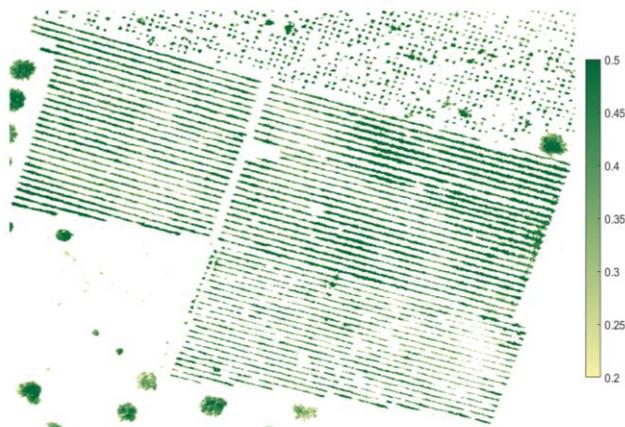
Figure 8. Zoomed view of the vigor map without the existence of soil.

(a)

(b)

Figure 9. Segmentation results for the area D as noted in Fig. 5. (a) Ground truth manually segmented image. (b) Visual representation of vine canopy segmentation using three distinct methods.

TABLE II. PERFORMANCE OF THE THREE ADOPTED METHODS IN TERMS OF ACCURACY

	HSV	Lab	ExG
Accuracy (%)	87.91	86.14	**91.08**

overall accuracy of the three adopted methods is depicted in Table II. Our evaluation shows that the incorporation of Excess Green Index presents an enhanced result for detecting the vine canopy with better accuracy.

B. Crop Row Detection

Hough Transformation (HT) is a widely used method for crop lines detection. At the same time, it is an essential technique for identifying discontinuous lines within crops leading to significant results about possible poor vegetation growth or missing plants. Hough Transform $H(\theta,\rho)$ was applied to the entire binary image for matching lines in the masked image. The vegetation mask has been resulted from Excess Green Index as described in previous subsection. Vegetation pixels were annotated with 1 and all the other information with 0. Each line is parameterized in terms of radius ρ which stands for the vertical distance from the origin of the image to that line and θ is the clock-wise inclination angle between the horizontal axis and the line ρ which is the line connecting the straight line with the origin as mentioned.

The set of (radius-angle) constitute each parametrized line [32]:

$$\rho = x \cdot \cos\theta + y\sin\theta \qquad (5)$$

The computed parameters ρ, θ are stored in a two dimensional accumulator array H(ρ,θ), which is a quantized space. Thus, each point (x_i, y_i) is transformed into a discretized (ρ, θ) curve and the accumulator cells which lie along this curve are incremented. Resulting peaks in the accumulator array represent strong evidence that a corresponding straight line exists in the image and the problem of crop line detection is deduced in local peak detection. Fig. 10 illustrates the detected crop rows and the Hough peaks of the previous oriented D area as in Fig. 9. Peaks are positioned around zero angle as expected and a couple of lines are over detected. It has to be mentioned that the point of view in Fig. 10 is the same as acquired from the UAV during flight campaign.

V. CONCLUSION AND FUTURE WORK

In this paper, techniques and algorithms that facilitate agricultural tasks were evaluated and the reported results provided information for extracting knowledge and identifying possible crop irregularities. The objective of this work's content aimed at the incorporation of different operations in order to alleviate farmers' and agriculturists' work and enhance their crop management and monitoring properties. Moreover, the material of this work comprises the basis stage of exploration, as a practical vineyard based survey, towards an integrated UAV based low-cost agricultural monitoring system. The smooth incorporation of
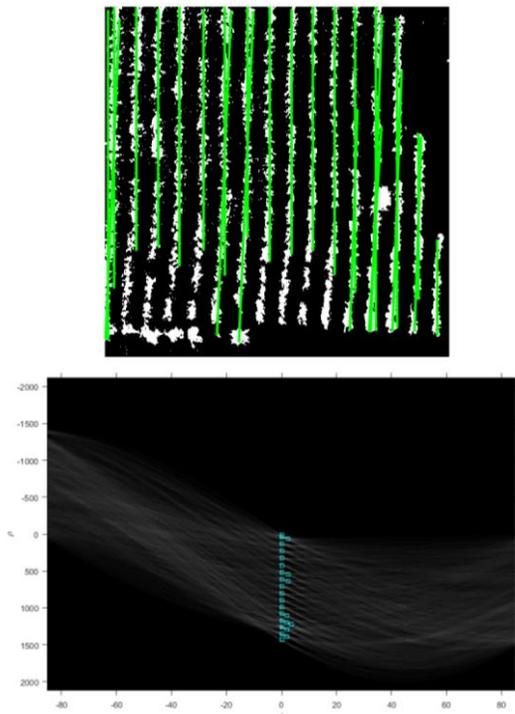

Figure 10. (upper) Crop rows detection. (lower) Hough peaks in the accumulator space with cyan squares.

UAVs in viniculture is particularly important especially for regions where there are indubitably identified needs. The described procedures are part of a work-in-progress and aim at an integrated framework that will provide multiple supportive utilities. Future work for improving and extending the overall established operational utilities will include classification tasks for crop/weed classification and possibly for diseases identification. Different descriptors such as Local Binary Patterns (LBPs) and Histogram of Oriented Gradients (HOG) as well as morphological texture descriptors will be taken into account. We expect that data fusion will produce a clear result capable of accurate classification.

REFERENCES

[1] R. Austin, *Unmanned Aircraft Systems. UAVs Design, Development and Deployment*, 1st ed. United Kingdom: John Wiley & Sons Ltd, 2010.

[2] N. Zhang, M. Wang, and N. Wang, "Precision agriculture—A worldwide overview," *Comput. Electron. Agric.*, vol. 36, nos. 2–3, pp. 113–132, Nov. 2002.

[3] D. J. Mulla, "Twenty five years of remote sensing in precision agriculture: Key advances and remaining knowledge gaps," *Biosyst. Eng.*, vol. 114, no. 4, pp. 358–371, Apr. 2013.

[4] L. Pádua, J. Vanko, J. Hruška, T. Adão, J. J. Sousa, E. Peres, and R. Morais, "UAS, sensors, and data processing in agroforestry: a review towards practical applications," *International Journal of Remote Sensing*, vol. 38, pp. 2349-2391, 2017.

[5] Q. L. Feng, J. T. Liu, and J. H. Gong, "UAV remote sensing for urban vegetation mapping using random forest and texture analysis," *Remote Sens.*, vol. 7, pp. 1074–1094, Jan. 2015.

[6] A. Matese, P. Toscano, S. F. Di Gennaro, L. Genesio, F. P. Vaccari, J. Primicerio, C. Belli, A. Zaldei, R. Bianconi, and B. Gioli, "Intercomparison of UAV, aircraft and satellite remote sensing platforms for precision viticulture," *Remote Sensing*, vol. 7, no. 3, pp. 2971–2990, 2015.

[7] A. S. Milas, M. Romanko, P. Reil, T. Abeysinghe, and A. Marambe, "The importance of leaf area index in mapping chlorophyll content of corn under different agricultural treatments using UAV images," *Int. J. Remote Sens.*, vol. 39, nos. 15–16, pp. 5415–5431, Mar. 2018.

[8] X. Zhou et al., "Predicting grain yield in rice using multi-temporal vegetation indices from UAV-based multispectral and digital imagery," *ISPRS Journal of Photogrammetry and Remote Sensing*, vol. 130, pp. 246–255, Aug. 2017.

[9] J. Torres-Sánchez, J. Peña, A. de Castro, and F. López-Granados, "Multitemporal mapping of the vegetation fraction in early-season wheat fields using images from UAV," *Comput. Electron. Agricult.*, vol. 103, pp. 104–113, Apr. 2014.

[10] L. Comba, P. Gay, J. Primicerio, and D. R. Aimonino, "Vineyard detection from unmanned aerial systems images," *Computers and Electronics in Agriculture*, vol. 114, pp. 78 – 87, 2015.

[11] International Organisation of Vine and Wine [OIV], "2019 Statistical Report on World Vitiviniculture", Available at: http:// http://www.oiv.int/public/medias/6782/oiv-2019-statistical-report-on-world-vitiviniculture.pdf.

[12] M. Weiss, F. Baret. Using 3D Point Clouds Derived from UAV RGBImagery to Describe Vineyard 3D Macro-Structure. *Remote Sens*, 9, 111, 2017.

[13] J. Navia, I. Mondragon, D. Patino, and J. Colorado, "Multispectral mapping in agriculture: Terrain mosaic using an autonomous quadcopter uav," in 2016 International Conference on Unmanned Aircraft Systems (ICUAS), June 2016, pp. 1351–1358.

[14] S. Candiago, F. Remondino, M. De Giglio, M. Dubbini, and M. Gattelli, "Evaluating multispectral images and vegetation indices for precision farming applications from UAV images," *Remote Sens.*, vol. 7, no. 4, pp. 4026–4047, 2015.

[15] J. Baluja et al., ''Assessment of vineyard water status variability by thermal and multispectral imagery using an unmanned aerial vehicle (UAV),'' *Irrigation Sci.*, vol. 30, no. 6, pp. 511–522, 2012.

[16] L. Luo, Y. Tang, X. Zou, C. Wang, P. Zhang, and W. Feng, "Robust grape cluster detection in a vineyard by combining the AdaBoost framework and multiple color components," *Sensors*, vol. 16, no. 12, art. no. 2098, 2016.

[17] S. Liu and M. Whitty, "Automatic grape bunch detection in vineyards with an SVM classifier," *J. Appl. Logic*, vol. 13, no. 4, pp. 643–653, Dec. 2015.

[18] R. Berenstein, O. Shahar, A. Shapiro, and Y. Edan, "Grape clusters and foliage detection algorithms for autonomous selective vineyard sprayer," *Intelligent Service Robotics*, vol. 3, no. 4, pp. 233–243, 2010.

[19] P. Tokekar, J. Vander Hook, D. Mulla, and V. Isler, "Sensor planning for a symbiotic UAV and UGV system for precision agriculture," *IEEE Trans. Robot.*, vol. 32, no. 6, pp. 1498–1511, 2016.

[20] C. Potena, R. Khanna, J. Nieto, R. Siegwart, D. Nardi, and A. Pretto, "AgriColMap: Aerial-ground collaborative 3D mapping for precision farming," *IEEE Robotics and Automation Letters*, vol. 4, no. 2, pp. 1085–1092, 2019.

[21] E. Galceran and M. Carreras, "A survey on coverage path planning for robotics," *Robotics and Autonomous Systems*, vol. 61, no. 12, pp. 1258–1276, 2013.

[22] B. Saha et al., ''Battery health management system for electric UAVs,'' *IEEE Aerosp. Conf.*, pp. 1–9, 2011.

[23] Y. Gabriely and E. Rimon, "Spanning-tree based coverage of continuous areas by a mobile robot," *Ann. Math. Artif. Intell.*, vol. 31, no. 1–4, pp. 77–98, 2001.

[24] J. P. Jarvis and D. E. White, "Computational experience with minimum spanning tree algorithms," *Operations Research Letters*, vol. 2, pp. 36-41, 1983.

[25] D.M. Woebbeck, G.E. Meyer, K. VonBargen, and D.A. Mortensen, "Color indices for weed identification under various soil, residue and lighting conditions", Trans. ASAE 38, USA, 1995, pp. 259-269.

[26] M. Louhaichi, M. M. Borman, and D. E. Johnson, "Spatially located platform and aerial photography for documentation of grazing impacts on wheat," *Geocarto International*, vol. 16, no. 1, pp. 65–70, 2001.

[27] C. J. Tucker, "Red and photographic infrared linear combinations for monitoring vegetation," *Remote Sens. Environ.*, vol. 8, pp. 127–150, 1979.

[28] G. Ruiz-Ruiz, J. Gómez-Gil, L.M. Navas-Gracia, "Testing different color spaces based on hue for the environmentally adaptive segmentation algorithm(EASA)," *Computers and Electronics in Agriculture*, vol 68, pp. 88–96, 2009.

[29] X. Bai, Z. Cao, Y. Wang, Z. Yu, Z. Hu, X. Zhang, et al., "Vegetation segmentation robust to illumination variations based on clustering and morphology modelling," *Biosystems Engineering*, vol. 125, no. 3, pp. 80–97, 2014.

[30] J. W. Rouse, Jr, R. H. Haas, J. A. Schell, and D. W. Deering, "Monitoring vegetation systems in the Great Plains with ERTS," Texas A&M Univ., College Station, TX, USA, Tech. Rep., 1974.

[31] N. Otsu, "A threshold selection method from gray-level histogram," *IEEE Trans. Syst., Man, Cybern.*, vol. 9, pp. 62–66, 1979.

[32] R. O. Duda and P. E. Hart, "Use of the hough transformation to detect lines and curves in pictures," *Communications of the Association for Comp. Mach.*, vol. 15, no. 1, pp. 11–15,1972.